International Journal of Remote Sensing
Vol. 29, No. 4, 20 February 2008, 1053–1073

Fire severity assessment by using NBR (Normalized Burn Ratio) and NDVI (Normalized Difference Vegetation Index) derived from LANDSAT TM/ETM images

S. ESCUIN*, R. NAVARRO and P. FERNÁNDEZ
†Department of Forestry Engineering, ETSI Agrónomos y Montes, University of Córdoba, Menéndez Pidal s/n, 14080 Córdoba, Spain

(*Received 30 July 2006; in revised form 10 February 2007*)

In this work, the capacity of NBR and NDVI indices derived from LANDSAT TM/ETM images has been analysed for fire severity assessment. For this purpose, three fires occurring in southern Spain were studied. Firstly, the displacements of burned and unburned pixels in the pre-/post-fire NIR-MIR and NIR-R bi-spectral spaces were analysed with the aim of establishing which of the two indices was the most sensitive for discriminating severity levels. Then, the capacity of the two indices, both from a uni-temporal (post-fire) and bi-temporal perspective (pre and post-fire), to discriminate three severity levels was studied. Based on the results, it was decided that the most suitable way to assess wildfire severity by index segmentation was to discriminate between unburned and burned pixels according to their NBR pre-/post-fire difference values (dNBR), and, subsequently, to distinguish between pixels with an extreme and moderate severity based on the NBR post-fire values. The thresholds calculated for these indices permitted fire severity mapping with an accuracy of 86.42% ($\pm$4.31%). These thresholds could be extrapolated to other fires with similar characteristics although a calculation of their own specific thresholds could improve the accuracy of the fire severity map obtained.

1. Introduction

In forest management it is essential to analyse the impact of a fire on the ecosystem. From a broad outlook, fire severity can be defined as the degree of change in the soil and vegetation caused by fire. Determining the perimeter of the fire, as well as the distribution of severity levels inside it, facilitates the process of making decisions aimed at restoring the affected areas. It also permits an analysis of fire effects on the post-fire vegetation succession.

It is difficult to map severity levels in large fires using traditional methods, especially when the affected area has a complex topography, with steep slopes, inaccessible areas and previous heterogeneous vegetation, all habitual circumstances in Mediterranean areas. After the fire, a series of spectrum changes takes place due to the fire consuming the vegetation, destroying the chlorophyll, leaving the soil bare, charring the roots and altering the soil's moisture. The reduction in chlorophyll results in an increase in the visible region of the electromagnetic spectrum and in a diminution in the near infra-red region. In addition, with the decrease in the tree canopy and soil moisture, the mid-infrared region increases after

*Corresponding author. Email: ir2esros@uco.es

International Journal of Remote Sensing
ISSN 0143-1161 print/ISSN 1366-5901 online © 2008 Taylor & Francis
http://www.tandf.co.uk/journals
DOI: 10.1080/01431160701281072

a fire event (Chuvieco 1997). For all those reasons, remote sensing, to be more specific, the analysis of LANDSAT TM/ETM images, constitutes a valuable tool for mapping burned areas and fire severity assessment as it offers an adequate spectral and spatial resolution. Among the techniques used to estimate the level of fire severity in vegetation, the indices derived from LANDSAT bands (ratios and normalized differences as well as pre-/post-fire temporal differences) stand out.

In several works, many of them done in the Mediterranean area, the capacity of indices combining the red and near-infrared regions to discriminate burned areas has been successfully tested. One of those most used, both from a uni-temporal (post-fire) and bi-temporal (pre-/post-fire difference) point of view has been NDVI (Normalized Difference Vegetation Index) (Viedma *et al.* 1997, Díaz-Delgado 1998, Pereira 1999, Vázquez *et al.* 1999, Quintano *et al.* 1999, Chuvieco *et al.* 2002, Heredia *et al.* 2003). In these works, it was argued that important falls in the values of this index are recorded with burned surfaces and that its segmentation could give a good approximation of the surface affected by a fire. Other indices combining the red and near-infrared regions used to a lesser extent are: BAI (Burnt Area Index) (Chuvieco *et al.* 2002, Heredia *et al.* 2003), SAVI (Soil Adjusted Vegetation Index) (Chuvieco *et al.* 2002) and GEMI (Global Environmental Index) (Periera 1999, Chuvieco *et al.* 2002).

The potential of the mid-infrared region of the spectrum for distinguishing burned areas has been used in works carried out in ecosystems as different as the African savannah (Trigg and Flasse 2001) and Mediterranean vegetation areas (Pereira 1999). The NBR (Normalized Burn Ratio) combining information on the near-infrared and the mid-infrared regions has been used in the discrimination of burned areas in the Mediterranean, using both a post-fire image (López *et al.* 1991, Heredia *et al.* 2003) and a bitemporal pre-/post-fire difference (Heredia *et al.* 2003). Like NDVI, NBR takes values ranging between -1 and 1. In vegetated areas it takes positive values, while its negative values correspond to bare soil. In burned areas, NBR values decline at the same time as the fire severity rises. NBR has been less used than NDVI in this type of study as it requires the availability of information on the mid-infrared region (band 7 in the TM/ETM sensors), which is lacking in some sensors frequently employed in these applications, like AVHRR and WIFS.

As for the distribution of severity levels inside the fire's perimeter, Diaz Delgado *et al.* (2003) found a positive correlation between the drop in NDVI index values and fire severity. Furthermore, in recent years, several works have demonstrated the relationship between the pre-/post-fire NBR difference (dNBR) and fire severity (Key and Benson 1999a, Wagtendonk *et al.* 2004, Cocke *et al.* 2005, Kokaly *et al.* 2006). In fact, dNBR, together with the fire severity assessment in-field index, Composite Burnt Index (CBI) (Key and Benson 1999b), is used at present operatively by the forestry services in the west of the USA (Howard and Lacasse 2004). Indeed, many works rely on dNBR to assess fire severity, which is later related to different aspects of vegetation evolution (Kotliar *et al.* 2003, Wimberly and Reilly 2005, Cocke *et al.* 2005). Epting *et al.* (2005) used 13 indices (bands, ratios, normalized differences) for the discrimination of fire severity levels in four fires in Alaska and concluded that post-fire NBR gave the best correlations with field damage, followed by dNBR. However, they warned that the relationship between the level of damage estimated and that assigned in-field was poorer in areas with a sparser tree cover (open woods, scrub and pastures). NBR, which, as mentioned above, has been used in Mediterranean areas for the discrimination of

burned areas and even for the monitoring of post-fire vegetation (López and Caselles 1991), but has not been employed for fire severity assessment. Recently, Roy *et al.* (2006) have questioned the usefulness of the NBR index, based on the results of their studies on the behaviour of the index using LANDSAT data sensed over South African savanna prescribed surface fires and MODIS sensed data over boreal and tropical forest fires. In this work, the NBR was seen to be fairly insensitive to the pre-/post-fire changes in the bi-spectral NIR-MIR space.

With regard to the advantages and drawbacks involved in the use of post-fire indices versus pre-/post-fire indices, it should be stressed that uni-temporal applications are cheaper and faster than bi-temporal ones. Additionally, bi-temporal applications imply a series of added errors derived from differences between images which are non-attributable to the fire but to geometric deficiencies, from the different illumination, atmospheric and phenological, etc., conditions, which it is necessary to minimize. To alleviate these effects, it is usual to co-register the images with a mean RMS of under 0.5 pixels and to carry out an atmospheric normalization between images; it is recommended that the pre-fire image and the post-fire image should be of the same date with a year's difference (Key and Benson 1999a). In opposition to this, it should be pointed out that one of the main disadvantages of using post-fire indices is that they do not give good results in the discrimination between burned areas and water surfaces or areas with bare soil or little vegetation (Heredia *et al.* 2003).

The researcher who analyses the evolution of vegetation in a burned area often has no information on the fire severity suffered by the vegetation immediately after the fire event. The application of supervised techniques (classification, regression, etc.), which requires a knowledge of the fire severity of a certain number of plots in the area, becomes complicated when it is a matter of studying fire events of past years, for which in-field information obtained in the weeks after the fire is scant or non-existent. Also, although the usefulness of the post-fire NDVI and NBR, as well as the respective bi-temporal indices (difference between the index value before and after the fire) dNDVI and dNBR in the discrimination of burned areas and fire severity has been proven with the results of the works mentioned, the ultimate challenge is to be able to generalize the results of some fires to others, at least in a regional context. This means controlling the "perturbing factors" which influence the spectral response observed and which are not related to the effect of the fire (Trigg and Flasse 2001), such as the illumination and atmospheric conditions. In this direction, some authors recommend using scenes close to the summer solstice, the moment at which the images show their best illumination conditions, with less shadow and where the contrast between the burned and unburned areas is more apparent (Key 2005). It is also necessary to take into account the intrinsic spectral characteristics of the surfaces analysed (type of vegetation affected and cover and its phenological state, moisture, soil, etc.), which will condition the pre-fire index value. Kokaly *et al.* (2006) warn about the impact of pre-fire cover on the use of dNBR to map fire severity. In order to assess the previous vegetation factor, Miller and Yool (2002), in a fire in New Mexico (USA), made a pre-classification of dNBR, thus improving the fire severity assessment results and demonstrating the importance of taking this factor into account.

The general aim of this work was to develop a methodology which permitted fire severity assessment from an analysis of the indices derived from LANDSAT TM/ETM images, NBR (Normalized Burn Ratio) and NDVI (Normalized Difference

Vegetation Index) both from a uni-temporal (post-fire) and bi-temporal (pre-/post-fire difference) perspective. This general objective was achieved by fulfilling three specific aims: (1) analysing the bi-spectral NIR-MIR and NIR-R displacements of pixels affected and unaffected by the fires and determining the optimality of the indices NBR and NDVI to assign the severity levels, (2) analysing the capacity for discriminating the severity levels of the following indices: NBR after the fire, NDVI after the fire, difference between the NBR index before and after the fire and difference between the NDVI index before and after the fire; (3) analysing the influence of the previous value of the indices on their behaviour, starting from the hypothesis that the decline in the NBR and NDVI indices values after a fire event depends both on severity and on the indices values before the fire, and (4) determining change thresholds in the fire severity level which could be generalized to other fires.

2. Materials and methods

2.1 *Study area*

The Environment Department of Andalusia (Southern Spain), in conjunction with the University of Cordoba, has conducted a burn severity assessment on all fires of over 200 ha which have occurred in forest land during the last 10 years. Based on this information, three fires were selected for this study (figure 1 and table 1). The

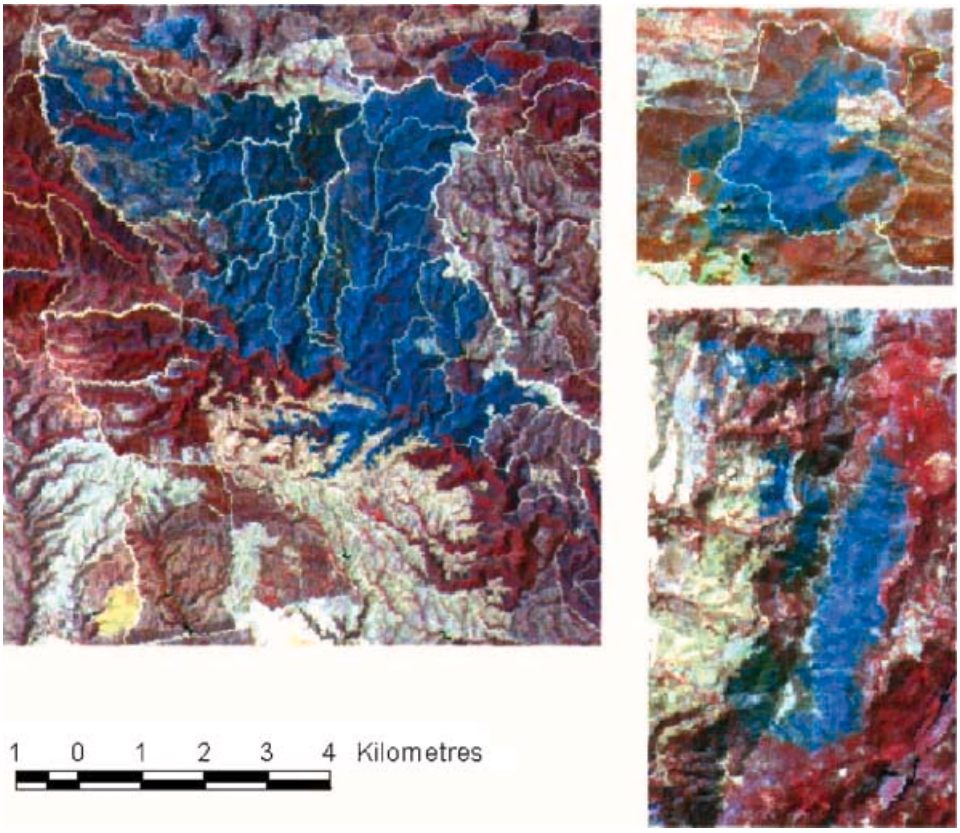

Figure 1. Post-fire 4-3-7 RGB LANDSAT images corresponding to the three study areas.

Table 1. Dates of the fires and pre-/post-fire images employed in the severity assessment study.

Fire	UTM X	UTM Y	Fire date	Pre-fire image	Post fire image
Aznalcóllar	203104	4162200	30/05/1995	20 Jul 1994	5 Jun 1995
Cazorla	505286	4201338	06/08/2001–08/08/2001	31 Aug 2000	3 Sep 2001
Nerva	187576	4183458	31/07/2001–03/08/2001	12 Jul 2000	1 Sep 2001

first fire occurred in Aznalcóllar (Seville) on May 30, 1995, affecting 2500 ha of stone pine (*Pinus pinea* L.) and cork oak (*Quercus suber* L.) forests, mixed with stands of eucalyptus (*Eucalyptus globulus* Labill.) and maritime pine (*Pinus pinaster* Aiton.). The elevation range is from 200 m to 450 m, with soils dominated by cambisols, eutric regosols and litosols predominating over slate, quartzite and schist. The second fire is located in Cazorla (Jaén) and was ignited on June 6, 2001, when it was extinguished three days later the fire had burned 800 ha of maritime pine and Aleppo pines (*Pinus halepensis* Mill.) forests. The elevation range is from 750 m to 1400 m with calcareous cambisols and regosols soils predominating over dolomites and limestone and, to a lesser extent, clays and loam. Finally, the third fire occurred in Nerva (Huelva) on 31 July, 2001 covering approximately 580 ha of stone pines, eucalyptus and small stands of maritime pine and Holm oak (*Quercus ilex* L. subsp. *ballota* (Desf.) Samp.). The elevation range is from 400 m to 700 m and eutric cambisols and umbric leptosol soils predominate over agglomerate, pumice, granite and slate. The selection of these three fires (from the large ones occurring in Andalusia between 1995 and 2001) was conditioned by the availability of images before and after the fire events, which met with our requirements with regard to their quality and to the dates necessary for carrying out this work. The affected areas were representative of the main tree-covered ecosystems in Andalusia so that the results could be extrapolated in the future to other fires in the region.

2.2 *Field work*

An initial assignation of damage was conducted on each fire in the weeks after the fire event (Key 2005) and, therefore, the field work and the acquisition of post-fire images were then carried out. The plots were established in *extreme* severity (total consumption or scorching of crowns), *moderate* severity (partial scorching of crowns) and *unburned* areas. Inside the perimeter of each fire, nine tree-covered plots with a *moderate* severity and nine with an *extreme* severity were located. Outside the fire perimeter, nine unburned plots were selected with a similar vegetation to that affected by the fire. The plots measured 90×90 m, the equivalent in LANDSAT scenes to a 3×3 pixel window. In Aznalcóllar, where the fire affected the largest surface, another nine plots were located per each severity level, which permitted a validation of the study results.

2.3 *Pre-processing of the images*

Table 1 shows the dates of the images employed in this work. They were selected in such a way that the date of the scene after the fire was the nearest to its occurrence, while the previous scene corresponded to one year earlier, with the aim of

minimizing the differences attributable to illumination conditions or phenological changes.

The images were subjected to the following pre-processing:

1. Geometrical correction, by the control points method, taking as a reference orthorectified aerial photographs of the area (1995–2001) with an RMS of under 0.5 píxels.
2. Conversion to reflectivity by the atmospheric correction method COST (Chavez 1996). An atmospheric correction was opted for and not a normalization between pre- and post-fire images as it was aimed at establishing comparisons between fires, not only between the corresponding differences in NBR and NDVI indices which took the pixels in each severity level, but also between the NBR_{post} and $NDVI_{post}$ values.
3. Generation of indices:

- NBR_{pre}: NBR corresponding to the scene before the fire
- NBR_{post}: NBR corresponding to the scene after the fire
- $NDVI_{pre}$: NDVI corresponding to the scene before the fire
- $NDVI_{post}$: NDVI corresponding to the scene after the fire
- $dNBR = NBR_{pre}\text{-}NBR_{post}$
- $dNDVI = NDVI_{pre}\text{-}NDVI_{post}$

where

$$NBR = 1000[(R_4 - R_7)/(R_4 + R_7)] \tag{1}$$

$$NDVI = 1000[(R_4 - R_3)/(R_4 + R_3)] \tag{2}$$

2.4 *Analysis of the pre-lpost-fire pixel displacements in the bi-spectral spaces NIR-MIR and NIR-R. Optimality of the indices NBR and NDVI*

In the NDVI or NBR spectral feature space, all the points of the equal index value (isolines) fall along straight lines passing through the origin. Ideally, if a spectral index is appropriate to the physical change of interest, then there is a simple relationship between the change and the direction of the displacement in the spectral feature space. The definition of an optimal spectral index requires the trajectory in the spectral feature space to be perpendicular to the index isolines (Verstraete and Pinty 1996). Figure 2 illustrates the optimal trajectory of a pixel from unburned to burned (vector UB_o), the real displacement from unburned to burned (vector UB) and the index isolines that pass through these values (Roy *et al.* 2006).

The real displacement of a burned pixel (vector UB) represents the spectral variation observed after the fire. The vector UB can be decomposed in the sum of the vectors UB_o and B_oB. The former, (UB_o), is related to the spectral changes to which the index (in this case NBR or NDVI) is sensitive, whereas, on the contrary, the latter (BoB) represents the spectral changes to which the index is not sensitive.

In this work, the displacements in the NIR-MIR and NIR-R bi-spectral spaces of the burned and unburned pixels correspond to the information in the plots acquired in the three fires. For each pixel, taking their pre- and post-fire spectral values, |UB| (spectral variation observed), $|B_oB|$ (spectral variation observed to which the index is

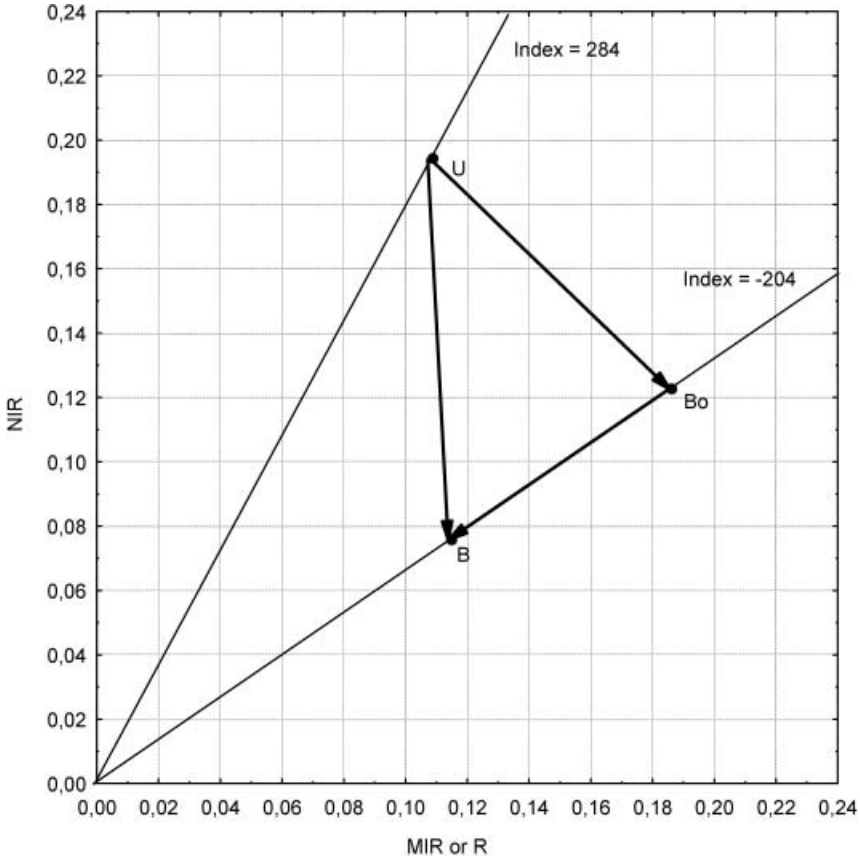

Figure 2. Example of the pre-/post-fire trajectory of a pixel in the NIR-MIR or NIR-R feature space. Isolines show the pre and post fire NBR or NDVI values (NBR if abscissa is MIR and NDVI if abscissa is R). Vector UB represents the real displacement of pixel after the fire, vector UB_o represents the displacements to which the index is sensitive and vector B_oB represents the displacement to which the index is not sensitive.

not sensitive) and $|UB_o|$ (spectral variation observed to which the index is sensitive) were calculated, and the optimality of the indices NBR and NDVI for detecting the pre-/post-fire spectral changes was calculated from the expression proposed by Roy *et al.* (2006):

$$\text{Optimality} = 1 - [|B_0B|/|UB|], \qquad 0 <= \text{Optimality} <= 1 \tag{3}$$

In the case of the index's behaviour being ideal, the optimality is equal to 1 and the spectral changes observed are perpendicular to the isolines of the index. If the index is completely insensitive to the spectral change, the optimality is 0 and the spectral changes are produced in the direction of the index isolines.

2.5 *Behaviour of the indices according to the severity level*

A study was made of the behaviour of the indices according to the severity levels in the three fires with the aim of detecting common features. For this purpose, an

exploratory analysis was carried out of the indices values presented by the pixels corresponding to the field plots.

It was predictable that for the same severity level the indices values were conditioned by their pre-fire NBR/NDVI values (that depended on the type of vegetation, cover, lithology, etc.). To analyse the effect of the prior value of the index, the following Pearson correlation coefficients were calculated: dNBR versus NBR_{pre}, NBR_{post} versus NBR_{pre}, dNDVI versus $NDVI_{pre}$, $NDVI_{post}$ versus $NDVI_{pre}$.

The capacity of the indices for discriminating severity levels was evaluated by estimating class separability by a calculation of the Jeffries–Matusita Distance (Swain and Davis 1978) which may range between 0 (there is no separability between classes) and 1414 (maximum separability).

2.6 *Determination of thresholds*

In terms of the results obtained in the optimality, separability and correlation analysis, the index with the greatest capacity for assessing fire severity was selected and its segmentation was carried out. To do this, it was necessary to determine the change thresholds between the *unburned-moderate* and *moderate-extreme* classes. These thresholds were determined in terms of the values of the index of each group of pixels according to their severity level for the group of fires so as to perceive the variability between them and enable the extrapolation of the results to other fires. The criterion of the multiple standard deviations was followed:

$$X_{\text{threshold}} = M_{\text{i}} \pm a\,\text{Devest}_{\text{i}} \tag{4}$$

- $X_{threshold}$: Index value corresponding to the threshold
- M_i: Mean class i
- a: constant
- $Devest_i$: Standard deviation of class i

The value of a, which some authors place at between 0.1 and 2 (Chuvieco 1996), can be determined iteratively in terms of the results.

2.7 *Validation*

Once the change thresholds were established, the segmentation of the index selected was performed for the fire with the greatest extension, Aznalcóllar, thus obtaining the fire severity map. Next, that map was validated with the field information from the 243 validation pixels, 81 pixels per class following the advice of Congalton (1991) who recommends a minimum of 50 pixels per class.

The validation pixels were located by means of a random cluster sampling. When a cluster sampling is carried out in remote sensing studies, it is recommended that they should not exceed 10 pixels (Congalton 1991) in order to prevent problems derived from spatial autocorrelation. For this work, nine clusters were located (validation plots) of 3×3 pixels for each severity level. The 27 validation plots were detected by a random cluster sampling, so that for each severity level nine plots with 3×3 pixels were located.

The corresponding error matrix was calculated in order to estimate the overall accuracy as the percentage of validation pixels whose class had been well assigned

with respect to the total number of validation pixels. Together with the overall accuracy, its confidence intervals for a 95% probability were calculated for each case, following equation (5) (Chuvieco 1996):

$$\text{Real accuracy} = \text{Overall accuracy} \pm 1.96\left[(pq)/n)^{0.5}\right] \tag{5}$$

p being the success percentage, q the failure percentage and n the number of pixels corresponding to the validation plots.

3. Results

3.1 *NBR and NDVI optimality*

Figures 3 and 4 show the mean and median values as well as the histograms of the optimality of the indices NBR and NDVI calculated separately for the unburned and burned pixels. Both the NBR and the NDVI present very low optimality values for pixels unaffected by the fire (means of 0.21 and 0.14). The bi-spectral displacements of these pixels are due to "perturbing factors", since severity is null in these pixels, so that the low optimality values indicate that both indices are hardly sensitive to these factors. For most of these pixels (74% in the NIR-MIR space and 84% in the NIR-R space), $|B_oB|$ which represents the spectral changes to which the index is not sensitive, is superior to $|UB_o|$, which represents the spectral changes to which the index is sensitive.

With regard to the burned pixels, the optimality values of the NBR are considerably higher, reaching a mean of 0.49. For most of these pixels (80%), $|UB_o|$ which represents the spectral changes to which the index is sensitive, is superior to $|B_oB|$, which represents the spectral changes to which the index is not sensitive.

The NDVI, however, has much lower optimality values (mean of 0.18), which indicates that the index is not sensitive to a good part of the displacement of the pixels corresponding to burned areas in the bi-spectral space. For the majority of the burned pixels (76%), $|B_oB|$ is superior to $|UB_o|$.

In accordance with these results, the NBR behaves more adequately than the NDVI for its use in fire severity applications.

3.2 *Indices' response to fire severity*

As was expected, in general, for a specific NBR_{pre}, the pixels with the lowest dNBR values correspond to the *unburned* class, the intermediate values to the *moderate* class and the pixels with the highest values of dNBR correspond to the *extreme* class (see figure 5). With regard to the correlations dNBR versus NBR_{pre}, no significant correlation ($p<0.01$) was detected in any of the three fires for the unburned class. Conversely, a positive and significant correlation did exist in the *moderate* and *extreme* classes although it should be pointed out that the correlation was weaker in the *moderate* class (r ranges between 0.31 and 0.56) than in the *extreme* class (r ranges between 0.77 and 0.91) (see table 2). The range of the index was 1177 points for Aznalcóllar, 1027 for Cazorla and 1036 points for Nerva (see table 3).

As for dNDVI, its behaviour was similar to that of the dNBR although in this case the range of the index was much smaller than that of the dNBR in the three fires (see table 3). The same as for the dNBR, in the dNDVI no significant correlations were detected with the $NDVI_{pre}$ in the pixels of the *not burned* class, while these correlations were significant for the *moderate* (with r values ranging

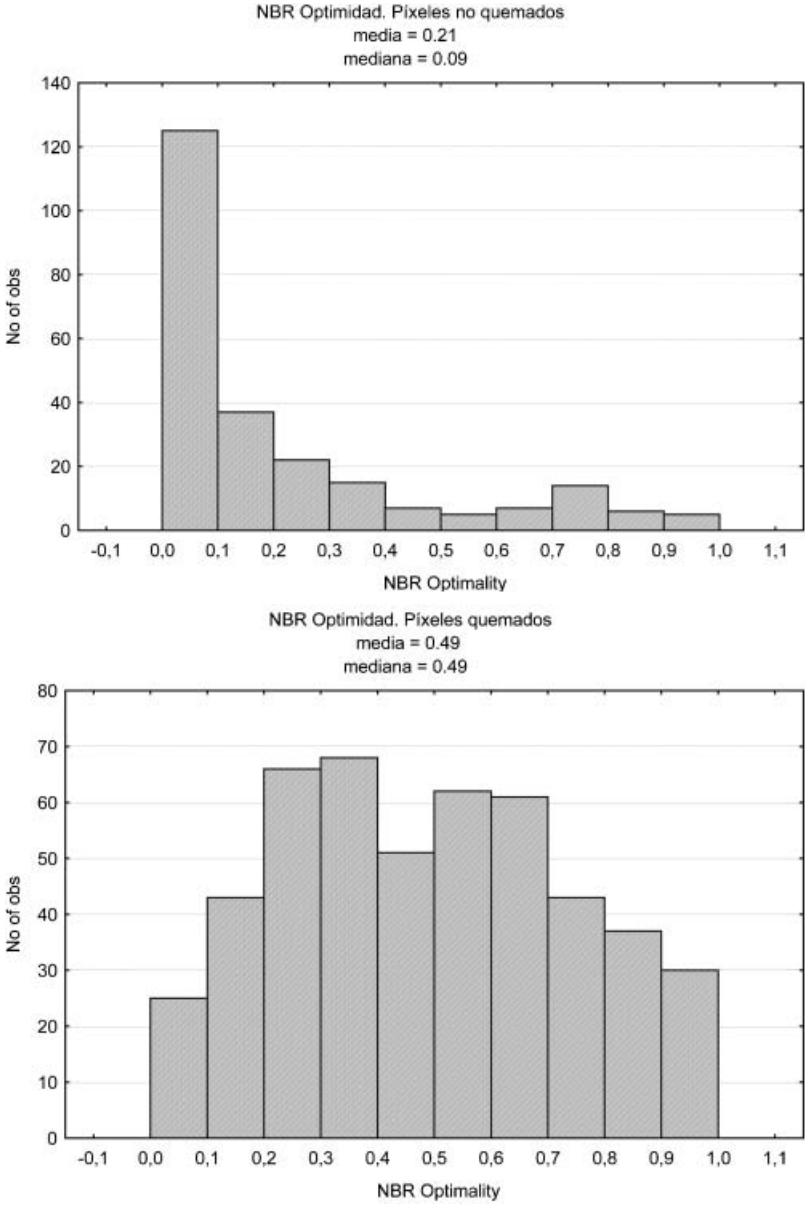

Figure 3. Histograms NBR Optimality computed from unburned and burned pixels of the three fires studied.

between 0.59 and 0.81) and *extreme* (with r values between 0.89 and 0.93) classes (see table 2).

With regard to NBR_{post}, the range was comparable to that of the dNBR (1041 points for Aznalcóllar and Cazorla and 1079 for Nerva, see table 3). For a same previous NBR value, the lowest values of NBR_{post} correspond to pixels with *extreme* class, the mean values to pixels with a *moderate* class and the highest values to *unburned* pixels. As for the correlations, the opposite situation occurs with respect to the bi-temporal indices. As expected, in the *unburned* pixels, NBR_{pre} and NBR_{post}

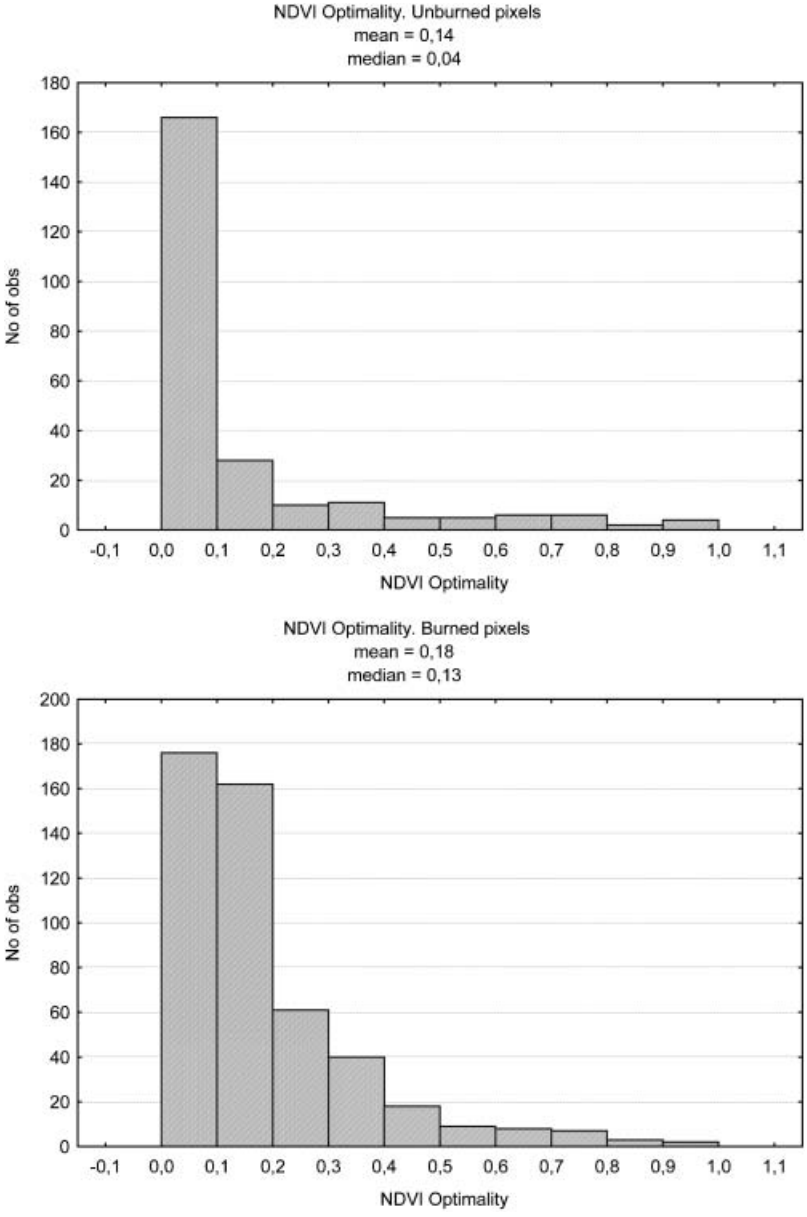

Figure 4. Histograms NDVI Optimality computed from unburned and burned pixels of the three fires studied.

were strongly correlated in the three fires with values of *r* ranging between 0.81 and 0.91. On the other hand, the *extreme* class pixels did not have any significant correlations while the *moderate* severity ones had significant correlations with *r* values ranging between 0.59 and 0.66 (see table 2)

Finally, the $NDVI_{post}$ showed a very similar behaviour to the NBR_{post} although the same as was observed in the bi-temporal indices, the amplitude was much smaller (see table 3). As for the correlations, they were again significant, with *r* between 0.84 and 0.90 for the *unburned* pixels and non-significant for the *extreme*

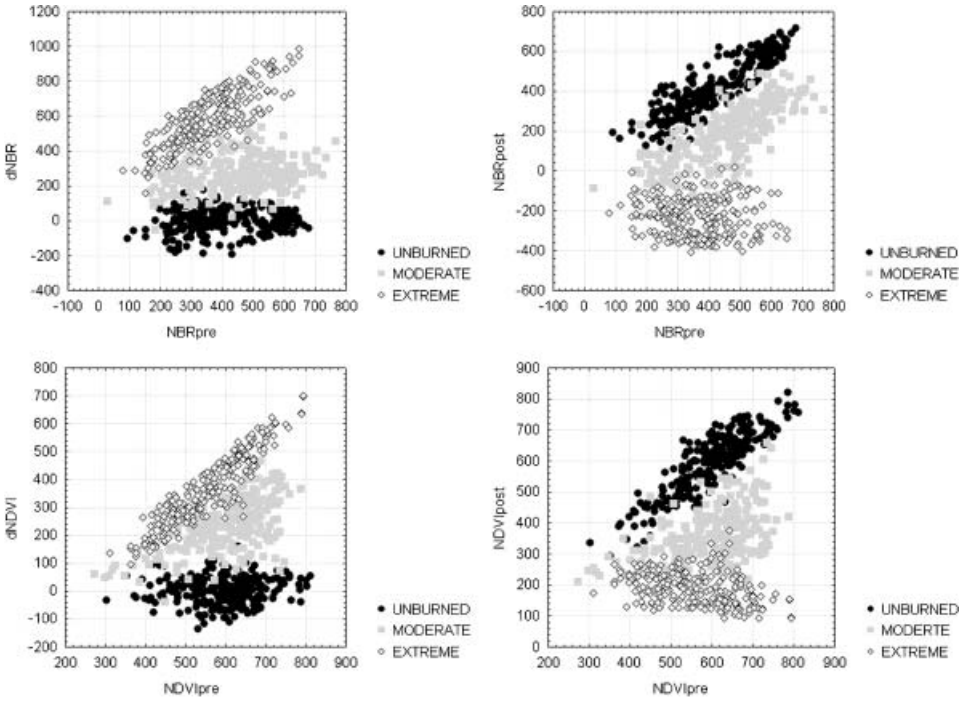

Figure 5. Scatter plots show a strong positive correlation NBR_{pre} versus dNBR and $NDVI_{pre}$ versus dNDVI for extreme fire severity pixels. On the other hand, a strong positive correlation NBR_{pre} versus NBR_{post} and $NDVI_{pre}$ versus $NDVI_{post}$ is detected for unburned pixels.

Table 2. Theoretical and observed ranges in each fire considering the pixels corresponding to the different severity levels jointly.

	Theoretical	Aznalcóllar	Cazorla	Nerva
dNBR	[−2000, +2000]	[−189, +988]	[−123, +904]	[−181, +855]
dNDVI	[−2000, +2000]	[−136, +700]	[−92, +463]	[−115, +603]
NBR_{post}	[−1000, +1000]	[−402, +639]	[−322, +719]	[−408, +671]
$NDVI_{post}$	[−1000, +1000]	[+93, +822]	[+155, +744]	[+101, +727]

Table 3. Pearson correlation coefficients between each index and its pre-fire value calculated for each fire (*$p<0.01$).

Fire	Severity level	dNBR v. NBR_{pre}	NBR_{post} v. NBR_{pre}	dNDVI v. $NDVI_{pre}$	$NDVI_{post}$ v. $NDVI_{pre}$
Aznalcóllar	Not burned	0.10	0.82*	0.23	0.88*
Cazorla	Not burned	−0.11	0.91*	−0.03	0.90*
Nerva	Not burned	0.11	0.81*	0.03	0.84*
Aznalcóllar	Moderate	0.31*	0.66*	0.59*	0.69*
Cazorla	Moderate	0.44*	0.66*	0.73*	0.28
Nerva	Moderate	0.56*	0.59*	0.81*	0.30
Aznalcóllar	Extreme	0.85*	−0.25	0.89*	−0.26
Cazorla	Extreme	0.91*	−0.05	0.93*	0.06
Nerva	Extreme	0.77*	−0.11	0.93*	−0.02

class pixels. The *moderate* class pixels had correlations but with highly variable *r* values ranging between 0.28 and 0.69 (see table 2).

Figures 6–8 show the values of the Jeffries–Matusita Distance (JM) for the *unburned-moderate, moderate-extreme* and *unburned-extreme* classes, calculated from the values displayed in table 4. In agreement with these values, the bi-temporal indices have a greater capacity for separating the *unburned-moderate* classes (figure 6). For these classes, dNBR presents higher JM values (of around 1200) than those of dNDVI in two of the three fires studied.

The results of the separability analysis between the *moderate* and *extreme* classes show that the greatest capacity for separating these classes corresponded to the NBR_{post}, followed by the $NDVI_{post}$. The results were clearly worse for the bi-temporal indices, although actually it was observed that the dNBR presented a better discrimination than the dNDVI (figure 7). Finally, the four indices had very high JM distance values between the *unburned* and *extreme* classes (figure 8).

It was observed that the indices with the worst separability results for two given classes were those which showed strong significant correlations for both classes (see

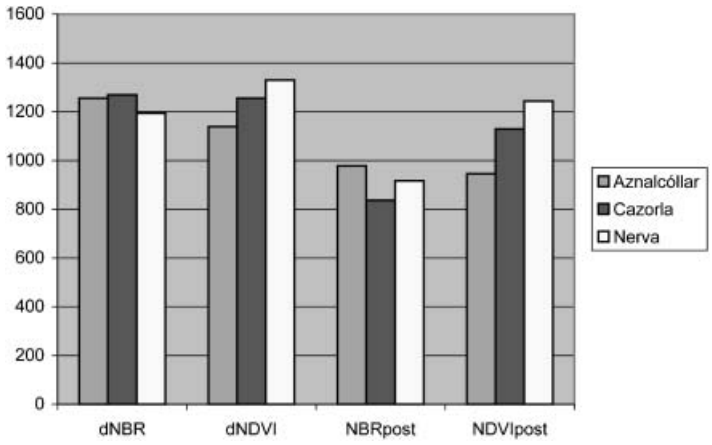

Figure 6. JM Distance values between *unburned-moderate* classes.

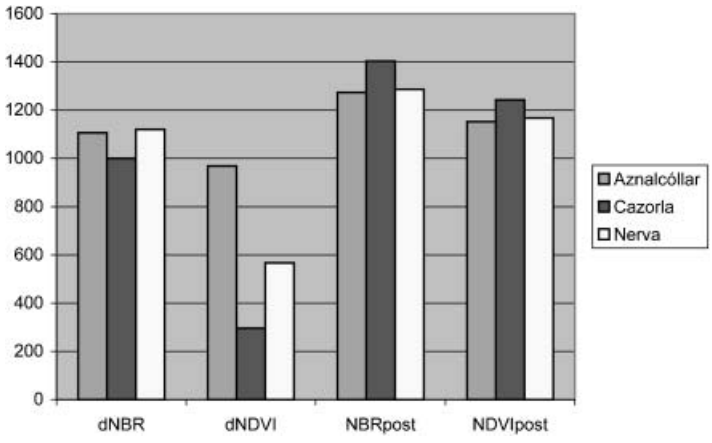

Figure 7. JM Distance values between the *moderate-extreme* values.

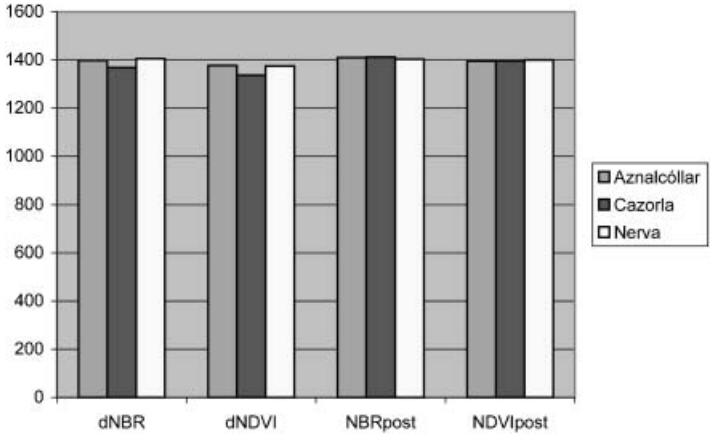

Figure 8. JM Distance values between the *not burned-extreme* values.

table 3). Thus, the post-fire indices (NBR_{post}, $NDVI_{post}$) gave worse results for the *unburned* and *moderate* classes, while the pre-/post-fire indices (dNBR, dNDVI) did so for the *extreme* and *moderate* classes. This was because in the classes with post- or pre-/post-fire index values significantly correlating with the previous values of the index, there was a greater dispersion and, therefore, a higher standard deviation (see table 4), which had an influence on the separability.

3.3 *Fire severity mapping*

The results of the analyses of the index behaviour according to the severity level demonstrated that pre-/post-fire indices are the most suitable for carrying out the discrimination between *unburned* and fire-*burned* pixels, while the post-fire indices were better for discriminating between pixels with a *moderate* and *extreme* severity. So, the combination of two indices, one pre-/post-fire and the other post-fire, i.e. the algorithm shown in figure 9, is considered to be the most appropriate solution for assigning severity levels.

Based on the results obtained in the above sections, the pre-/post-fire index chosen was the dNBR and the post-fire one the NBR_{post}. Then, threshold 1 (dNBR value

Table 4. Mean values and standard deviation for the pixels studied according to severity level and fire.

		dNBR	dNDVI	NBRpost	NDVIpost
Fire	Severity level	Mean (SD)	Mean (SD)	Mean (SD)	Mean (SD)
Aznalcóllar	Not burned	26 (68)	−1 (53)	383 (118)	621 (106)
Cazorla	Not burned	−3 (54)	−3 (42)	519 (129)	604 (95)
Nerva	Not burned	−30 (75)	9 (51)	364 (127)	558 (92)
Aznalcóllar	Moderate	318 (97)	205 (89)	107 (124)	397 (100)
Cazorla	Moderate	243 (81)	216 (81)	312 (97)	386 (58)
Nerva	Moderate	265 (111)	293 (84)	111 (115)	308 (52)
Aznalcóllar	Extreme	661 (152)	438 (119)	−272 (82)	167 (56)
Cazorla	Extreme	510 (152)	265 (81)	−158 (63)	236 (29)
Nerva	Extreme	612 (136)	401 (106)	−270 (88)	172 (38)

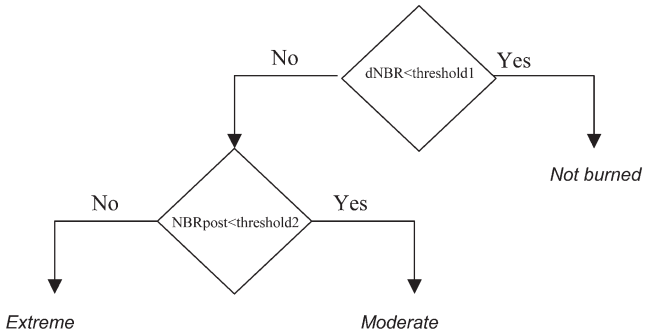

Figure 9. Algorithm for fire severity assessment by means of index segmentation.

which would permit the separation of the *unburned* pixels from the rest) and threshold 2 (NBR_{post} value allowing the separation of the *moderate severity* pixels from those with *extreme* severity) were determined for the group of fires in order to take into account the differences between fires and enable the extrapolation of their results to other fires.

The mean dNBR value and standard deviation of the *unburned* pixels for the three fires was -2 ± 69. However, the mean NBR_{post} value and standard deviation of the pixels with an *extreme* severity, for the group of fires, was -233 ± 95. Starting from these values, an iterative process was followed in which the successive standard deviation multiples were added to the means until the thresholds calculated gave rise to a success percentage of over 95% in the two classes to be separated (see tables 5 and 6).

The threshold obtained for separating the *unburned* and *moderate* classes was dNBR = 107 points. That obtained for separating the *moderate* and *extreme* classes was $NBR_{post} = -73$. In agreement with the algorithm in figure 9, 94.65% of the pixels were correctly assigned to their class (95.88% of the *unburned* pixels, 92.18% of the *moderate* class pixels and 95.88% of the *extreme* class pixels).

Taking the dNBR and NBR_{post} scenes corresponding to the Aznalcóllar fire, with the thresholds calculated for the group of fires and following the schema in figure 9, the severity levels were mapped. This map was validated with the group of pixels corresponding to the validation plots of the Aznalcóllar fire. The error matrix obtained is shown in table 7. The overall accuracy, namely the percentage of well classified validation pixels, was 84.42%.

Table 5. Determination of the dNBR threshold between the *unburned* and *moderate* classes by the standard deviation multiple method.

		Not burned	mMderate
Iteration	Threshold dNBR	% well classified	% well classified
1SD	67	85.60	99.18
2SD	137	97.94	92.59
1.5SD	102	93.83	95.88
1.75SD	120	97.12	93.83
1.625SD	111	96.30	94.65
1.5625SD	107	95.88	95.47

Table 6. Determination of the NBR_{post} threshold between the *moderate* and *extreme* classes by the standard deviation multiple method.

		Moderate	Extreme
Iteration	Threshold NBR_{post}	% well classified	% well classified
1 SD	−138	100.00	82.30
2 SD	−44	92.59	97.94
1.5 SD	−91	98.35	92.18
1.75 SD	−67	94.65	96.30
1.625 SD	−79	97.53	94.24
1.6875 SD	−73	96.71	95.88

4. Discussion

The results of the analysis of the pre-/post-fire bi-spectral displacements (NIR-MIR and NIR-R) of the pixels unaffected by the fire demonstrated that both indices, NBR and NDVI, were hardly sensitive to the spectral changes caused by "perturbing factors", which is positive with regard to their use in assigning post-fire severity. The results corresponding to pixels affected by the fire (with a moderate or extreme severity) show that the NBR is much more sensitive than the NDVI to the spectral changes produced. Although the optimality of the NBR calculated for this group of pixels (mean of 0.49) is below the ideal, it was observed that the displacements of 80% of the pixels followed a trajectory nearer to the perpendicular at the index isolines (ideal trajectory), which paralleled them. This was a manifestation of the usefulness of this index for assigning severity levels with LANDSAT. These results contrast with those obtained by Roy *et al.* (2006), who report very low NBR optimality values (mean of 0.1) calculated with LANDSAT for a very specific type of fire, i.e. burning of surface in the African savannah, these being difficult to extrapolate to fires on treetops in tree-covered areas. The same authors obtain very low NBR optimality values for other ecosystems like boreal or tropical forests, but in these cases optimality is calculated as an average of a group of MODIS pixels, including both burned and unburned pixels. According to the results of this present work, the NBR is fairly insensitive to the pre-/post-fire changes in unburned pixels and, therefore, it would seem reasonably probable that the poor mean optimality results obtained by Roy *et al.* (2006) were due to the fact that pixels unaffected by the fire were included in their calculation.

The sensitivity to fire severity that dNBR, NBR_{post}, dNDVI and $NDVI_{post}$ showed in this work coincide with that described by other authors (Key and Benson 1999a, 1999b, Díaz Delgado *et al.* 2003, Wagtendonk *et al.* 2004, Epting *et al.* 2005). However, one should point out the greater capacity of the NBR to assess fire severity levels, which is in agreement with the results of previous works that

Table 7. Error matrix (%) corresponding to the validation pixels.

GA	Not burned (estimated)	Moderate (estimated)	Extreme (estimated)
Not burned	91.36	8.64	0.00
Moderate	0.00	77.78	22.22
Extreme	0.00	9.88	90.12

Global accuracy: 84.42%
Real accuracy: 84.42 +/−4.31%

compare NBR and NDVI (Key *et al.* 1999, Pereira 1999, Heredia 2003, Epting 2005). The Introduction section contains the advantages and disadvantages of the use of post-fire indices compared to difference pre-/post-fire indices observed by different authors. Based on the results of this work, it should be added that since the pre-/post-fire indices were significantly correlated with the pre-fire index value when the severity level was *moderate* to *extreme* and given that the post-fire indices were significantly correlated with the previous index value when the severity level was *not burned* to *moderate*, it would not be advisable to use one or the other for assigning severity levels independently without taking into account the pre-fire value. Based on the observation of the indices' behaviour, in order to assess fire severity levels by means of indices segmentation, it is recommended to employ a combination of a pre-/post-fire index (preferably dNBR), which discriminates between *unburned* pixels and the rest, with the post-fire index (preferably NBR_{post}), which discriminates between *extreme* and *moderate* severity.

The mean values of the indices in the different fires for the same severity level differed, in some cases remarkably, from one fire to another. It is likely that the most notable differences between fires, and even in the same fire, for the pixels corresponding to the same severity level were due to the mentioned effect on the previous index value (which, in turn, depends on the type of vegetation, moisture, soil type, lithology, etc.). The methodology proposed eliminates this effect because the threshold separating the *unburned* pixels from the rest was calculated on the basis of their dNBR values, which were not correlated with their respective NBR_{pre} values. Analogously, the threshold separating the *extreme* severity pixels from the *moderate* ones was calculated based on the NBR_{post} of the *extreme* pixels, which were not correlated with their respective NBR_{pre} values.

Other factors which, although attempts were made to minimize them, were not completely controlled and may have an influence on the behaviour differences of the indices from one fire to another are: deficiencies in the pre-processing of the images (geometric corrections, errors in the atmospheric correction model employed), or differences due to the moment of the acquisition of the images, which made the time lapses acquisition of previous image-acquisition of subsequent image, field work execution-acquisition of subsequent image be variable between fires. In any case, as already mentioned, neither NBR nor NDVI were not seen to be very sensitive to the spectral changes produced in unburned pixels by these "perturbing factors".

Furthermore, it should be remembered that fire severity is actually a continuous variable, the same as the spectral response of the plant cover affected. The discrete classes defined in this work include a really wide range of possibilities, which lend importance to the variability in the index value for the same severity level in each fire and between fires, depending on the type of combustion, soil characteristics, lithology, etc. As an example of this, figure 10 shows the NBR_{post} values of the pixels with an *extreme* severity level for each fire differentiating those pixels in which no burned remains of foliage remained on the branches (total consumption of crowns) and those in which these did appear (scorched crowns) (in Cazorla, in all the plots). It can be clearly observed that in the plots in which a total combustion of the foliage took place, the NBR_{post} was lesser regardless of which fire it was.

In any event, these uncontrolled factors did not prevent reaching a dNBR threshold (107) which permitted the separation of the *unburned* pixels from the rest and a NBR_{post} (-73) threshold permitting the separation of *moderate* severity pixels from the *extreme* pixels with 94.65% of well-classified pixels. By applying these

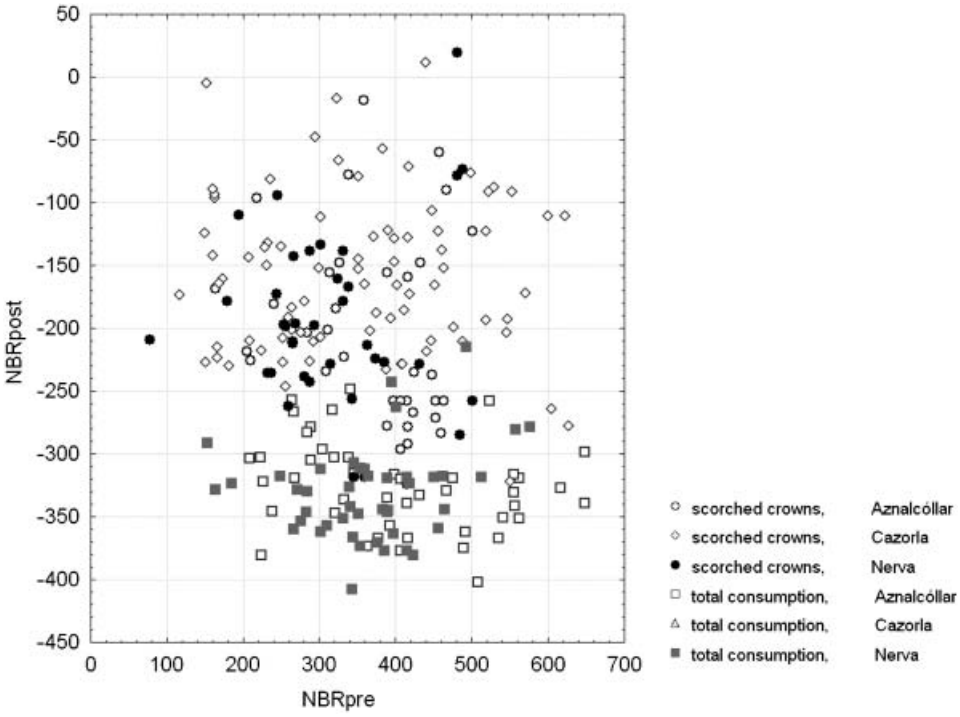

Figure 10. Scatterplot NBR_{post} versus NBR_{pre} for the pixels with an extreme severity differentiating if they corresponded to plots with remains of burned foliage on the crowns (scorched crowns) or plots with crowns totally burned (total consumption).

thresholds to the Aznalcóllar fire, its severity levels were mapped and its validation gave a global accuracy of 86.42% and a real accuracy of $86.42 \pm 4.31\%$. These results are slightly higher than those reported for forested areas by Epting *et al.* (2005) and Cocke *et al.* (2005), who, when considering three and four severity levels by means of a segmentation of the dNBR, obtained a global accuracy of 80.77% and 75%, respectively.

The question to be asked is whether the thresholds calculated in this work can be used to assess fire severity in other fires different from those analysed here. In this sense, it should be pointed out that the dNBR = 107 points threshold established to separate the *unburned* pixels from those with a *moderate* severity is very near to the orientative threshold fixed by Key *et al.* (2005) at dNBR = 100 points and that which Epting *et al.* (2005) arrived at, dNBR = 90 points, for one of the fires studied in their works. No specific data were found in the literature on NBR_{post} threshold values according to severity levels, but, however, the NBR_{post} was analysed for two other fires in Andalusia, southern Spain: Quesada, occurring in 2000, and Ojén in 1999. It was verified that in the Quesada fire, which affected masses of Aleppo pines, 97.53% of the pixels corresponding to *extreme* class plots had NBR_{post} values of under -73 and 96.30% of the pixels corresponding to *moderate* class plots gave values of over -73. In Ojén, a fire which mainly affected shrubs and dispersed tree clumps, 77.78% of the pixels corresponding to *extreme* class plots displayed values of under -73 and 85.56% of the pixels corresponding to *moderate* class plots had values of over -73. All this leads one to assume that these thresholds are extrapolable to other fires, even those which have affected clumps of dispersed trees or scrub.

5. Conclusions

The NBR index showed itself to be more sensitive to the pre-/post-fire displacements of the pixels affected by the fire in the MIR-NIR space than the NDVI in the R-NIR space. Both indices were hardly sensitive to the pre-/post-fire spectral changes corresponding to the unaffected pixels attributable to "perturbing factors". The pre-/post-fire difference indices dNBR and dNDVI are the most suitable ones for carrying out the discrimination between pixels *not burned* by a fire (whose values are not significantly correlated with the previous values of the indices) and pixels affected by a fire. dNBR displayed slightly better results than dNDVI for separating the *unburned-moderate* classes. However, the post-fire indices NBR_{post} and $NDVI_{post}$ are better for discriminating between *extreme* severity pixels (whose values are not significantly correlated with the previous values of the indices) and pixels with a *moderate* severity. The NBR_{post} gave clearly better results than $NDVI_{post}$ for the severity between the *moderate-extreme* classes.

The dNBR and NBR_{post} indices presented a clearly higher range than the dNDVI and $NDVI_{post}$ indices, which suggests that they are more suitable for detecting different severity levels. The best option for assessing fire severity by the segmentation of the indices studied is to do so in two steps: (1) separating the *unburned* pixels from the rest on the basis of their dNBR value, (2) separating the *extreme* severity pixels from the *moderate* severity ones based on their NBR_{post} value.

In this work, the following thresholds were determined for fire severity assessment: *unburned* pixels if $dNBR<107$ and pixels with an *extreme* severity if $NBR_{post}<-73$. These thresholds can be extrapolated to other fires although the calculation of the latter's own thresholds, whenever possible, would improve the accuracy of fire severity maps.

Acknowledgements

Thanks are given to the Environmental Department of Andalucía (Andalucía, Spain) for financial support.

References

CHÁVEZ, P.S., 1996, Imaged-based atmospheric corrections. Revised and improved. *Photogrammetric Engineering & Remote Sensing*, **9**, pp. 1025–1036.

CHUVIECO, E., 1996, *Fundamentos de teledetección espacial*, pp. 568 (Madrid: Ediciones Rialp).

CHUVIECO, E. (Ed), 1997, *Remote Sensing of Large Wildfires in the European Mediterranean Basin* (Berlin: Springer-Verlag).

CHUVIECO, E., MARTÍN, M.P. and PALACIOS, A., 2002, Assessment of different spectral indices in the red-near-infrared spectral domain for burned land discrimination. *International Journal of Remote Sensing*, **23**, pp. 5103–5110.

COCKE, A.E., FULÉ, P.Z. and CROUSE, J.E., 2005, Comparison of burn severity assessments using Differenced Normalized Burn Ratio and ground data. *International Journal of Wildland Fire*, **14**, pp. 189–198.

CONGALTON, R.G., 1991, A review of assessing the accuracy of classifications of remotely sensed data. *Remote Sensing of Environment*, **37**, pp. 35–46.

DÍAZ-DELGADO, R., 1998, Detección de superficies quemadas en Cataluña mediante imágenes de satélite durante el período 1975–1995. Aplicación para la caracterización del régimen de incendios y los procesos de regeneración de la vegetación. *Serie Geográfica*, **7**, pp. 239–137.

DÍAZ-DELGADO, R., LLORET, F. and PONS, X., 2003, Influence of fire severity on plant regeneration by means of remote sensing imagery. *International Journal of Remote Sensing*, **8**, pp. 1751–1763.

EPTING, J., VERBYL, D. and SORBEL, B., 2005, Evaluation of remotely sensed indices for assessing burn severity in interior Alaska using Landsat TM and ETM+. *Remote Sensing of Environment*, **96**, pp. 228–239.

HEREDIA, A., MARTÍNEZ, S., QUINTERO, E., PIÑEROS, W. and CHUVIECO, E., 2003, Comparación de distintas técnicas de análisis digital para la cartografía de áreas quemadas con imágenes Landsat TM. *Geofocus*, **3**, pp. 216–234.

HOWARD, S.M. and LACASSE, M.L., 2004, An evaluation of Gap-Filled Landsat SLC-Off imagery for wildland fire burn severity mapping. *Photogrammetric Engineering and Remote Sensing*, **70**, pp. 877–879.

KEY, C.H. and BENSON, N.C., 1999a, The Normalized Burn Ratio, a Landsat TM radiometric index for burn severity. Available online at: http://nrmsc.usgs.gov/research/nbr.htm. (accessed 10/2001).

KEY, C.H. and BENSON, N.C., 1999b, A general field method for rating burn severity with extended application to remote sensing. Available online at: http://nrmsc.usgs.gov/research/cbi.htm (accessed 10/2001).

KEY, C.H., 2005, Remote sensing sensitivity in fire severity and fire recovery. *Proceedings of the 5th International Workshop on Remote Sensing and GIS Applications to Forest Fire Management Zaragoza (Spain)*. Fire Effects Assessment: pp. 29–39.

KOKALY, R.F., ROCKWELL, B.W., HAIRE, S.L. and KING, T.V.V., 2006, Characterization of post-fire surface cover, soils, and burn severity at the Cerro Grande Fire, New Mexico, using hyperspectral and multispectral remote sensing. *Remote Sensing of Environment*, **106**, pp. 305–325.

KOTLIAR, N.B., HAIRE, S.L. and KEY, C.H., 2003, Lessons from fires of 2000. Post-fire heterogeneity in ponderosa pine forests. *USDA Forest Service Proceedings* RMRS-P29.

LÓPEZ, M.J. and CASELLES, V., 1991, Mapping burns and natural reforestation using Thematic Mapper data. *Geocarto International*, **1**, pp. 31–37.

MILLER, J.D. and YOOL, S.R., 2002, Mapping post-fire canopy consumption in several overstory types using multi-temporal Landsat TM and ETM data. *Remote Sensing of Environment*, **82**, pp. 481–496.

PEREIRA, J.M., 1999, A comparative evaluation of NOAA AVHRR vegetation indices for Burned Surface Detection and Mapping. *IEEE Transactions on Geoscience and Remote Sensing*, **37**, pp. 217–226.

QUINTANO, E., DELGADO, J.A., FERNÁNDEZ, A. and ILLERA, P., 1999, Cartografía automática de grandes incendios forestales con imágenes Landsat. *VIII Congreso de Teledetección, Albacete (Spain)*.

ROY, D.P., BOSCHETTI, L. and TRIGG, S.N., 2006, Remote sensing of fire severity: assessing the performance of the Normalized Burn Ratio. *IEEE Geoscience and Remote Sensing Letters*, **1**, pp. 112–116.

SWAIN, P.H. and DAVIS, S.M., 1978, *Remote Sensing: The Quantitative Approach* (New York: McGraw Hill Book Company).

TRIGG, S. and FLASSE, S., 2001, An evaluation of different bi-spectral spaces for discriminating burned shrub-savannah. *International Journal of Remote Sensing*, **13**, pp. 2641–2647.

VÁZQUEZ, A., CUEVAS, J.M. and GONZÁLEZ-ALONSO, F., 1999, Evaluación de la superficie afectada por el gran incendio de Cataluña Central de 1998 a partir de imágenes LISS-III y WIFS. *Revista de Teledetección*, **12**, pp. 1–4.

VERSTRAETE, M.M. and PINTY, M., 1996, Designing optimal spectral indexes for remote sensing applications *IEEE Transactions on Geoscience and Remote Sensing*, **5**, pp. 1254–1265.

VIEDMA, O., MELIÁ, J., SEGARRA, D. and GARCÍA-HARO, J., 1997, Modeling rates of ecosystem recovery after fires using Landsat TM data. *Remote Sensing of Environment*, **61**, pp. 383–398.

WAGTENDONK, J.W., ROOT, R.R. and KEY, C.H., 2004, Comparison of AVIRIS and Landsat ETM+ detection capabilities for burn severity. *Remote Sensing of Environment*, **92**, pp. 397–408.

WIMBERLY, M.C. and REILLY, M.J., 2005, Using satellite imagery to map fire severity and forest community change in the southern Appalachians. *EastFIRE Session*, Available online at: http://www.comet.ucar.edu/outreach/EastFIREConfProc/Abstracts/Session%201C%20PDF/1C_Wimberly.pdf (accessed 10/2005).

Copyright of International Journal of Remote Sensing is the property of Taylor & Francis Ltd and its content may not be copied or emailed to multiple sites or posted to a listserv without the copyright holder's express written permission. However, users may print, download, or email articles for individual use.